

# Finite-Temperature Phase Diagram of Quasi-One-Dimensional Molecular Conductors: Quantum Monte Carlo Study

Yuichi OTSUKA<sup>1,2\*</sup>, Hitoshi SEO<sup>2</sup>, Yukitoshi MOTOME<sup>3</sup>, and Takeo KATO<sup>4</sup>

<sup>1</sup> CREST, Japan Science and Technology Agency, Kawaguchi, Saitama 332-0012

<sup>2</sup> Synchrotron Radiation Research Center, Japan Atomic Energy Agency, SPring-8, Hyogo 679-5148

<sup>3</sup> Department of Applied Physics, University of Tokyo, Hongo Bunkyo-ku, Tokyo 113-8656

<sup>4</sup> Institute for Solid State Physics, University of Tokyo, Kashiwa, Chiba 277-8581

Finite-temperature phase transitions in quasi-one-dimensional quarter-filled systems are investigated using the extended Hubbard model with electron-lattice coupling. By a quantum Monte Carlo method combined with interchain mean-field approximation, we clarify competing and coexisting behaviors among charge ordering, dimer Mott, and spin-Peierls states. It is pointed out that an anharmonicity of lattice distortions plays an important role in multicritical behaviors. The results are compared with experimental data for quasi-one-dimensional molecular conductors such as DCNQI and TMTTF compounds.

**KEYWORDS:** quasi-one-dimensional molecular conductors, extended Hubbard model, electron-lattice coupling, charge ordering, lattice dimerization, spin-Peierls transition, SSE Monte Carlo method

Quasi-one-dimensional (Q1D) molecular conductors have been recognized as materials suitable for studying the effects of strong correlation. In these compounds, Coulomb interaction and enhanced fluctuations due to low dimensionality give rise to keen competitions in charge, spin, and lattice degrees of freedoms. As a result, they show various phase transitions despite the fact that their noninteracting band structures are often very similar.<sup>1</sup>

A typical case is the family of  $(R_1R_2\text{-DCNQI})_2X$  ( $R_1, R_2$ : substituents,  $X$ : monovalent cation). The electronic structure is commonly described by a Q1D quarter-filled  $\pi$ -band of DCNQI chains,<sup>2</sup> whereas their physical properties depend strongly on  $R_1, R_2$ , and  $X$ . For instance, DI-DCNQI<sub>2</sub>Ag shows a charge-ordering (CO) phase transition at  $T = 220$  K and an antiferromagnetic transition at 5 K.<sup>3,4</sup> On the other hand, DMe-DCNQI<sub>2</sub>Ag exhibits, instead of CO, lattice dimerization at  $T = 100$  K, which drives the system effectively half-filled, resulting in a dimer Mott (DM) insulating state. Furthermore, tetramerization occurs at  $T = 80$  K, which is ascribed to a spin-Peierls (SP) transition.<sup>5</sup> Such a variety of properties suggests a subtle balance among different phases under electron correlation.

Another good example is found in  $(\text{TMTTF})_2X$  ( $X$ : monovalent anion), whose Q1D  $\pi$ -band of TMTTF chains is quarter-filled in terms of holes.<sup>6</sup> In contrast to the DCNQI systems, an intrinsic dimerization exists along the chains from the outset. These compounds also exhibit rich phases depending on  $X$ . The CO transition occurs at around 100 K, which is followed by a SP transition at a lower temperature ( $T$ ) for  $X = \text{PF}_6$  and  $\text{AsF}_6$  or an antiferromagnetic transition for  $X = \text{SbF}_6$ .<sup>7-9</sup> For  $X = \text{AsF}_6$ , the CO phase is suppressed under applied pressure ( $P$ ), while the SP state persists up to higher  $P$ . This indicates that the CO and SP states are competing in nature.<sup>8</sup>

Theoretically, correlation effects in such Q1D molecular conductors have been studied using the 1D or Q1D quarter-filled extended Hubbard model with on-site and intersite Coulomb interactions, mainly focusing on the ground state.<sup>10</sup> Several studies have recently been conducted to describe their finite- $T$  properties.<sup>11-16</sup> In such studies, it is crucial to treat 1D electronic fluctuations properly, which originate from the strong electron correlation. This is because development of correlation lengths is strongly anisotropic along 1D chains, which finally results in phase transitions through interchain interaction or coupling to the three-dimensional lattice. Moreover, the paramagnetic insulating nature in strongly correlated phases such as the CO and DM states can be captured only when the fluctuation effects are taken into account. Recently, a numerical study including such 1D fluctuation effects was performed<sup>14</sup> using the quantum transfer-matrix (QTM) method combined with the interchain mean-field approximation. Although competitions among different phases were elucidated, the low- $T$  region was not fully investigated because of limitations of the QTM method. Most of the intriguing competitions in real materials appear at much lower  $T$ ; hence, it is strongly desired to study the low- $T$  region to understand the experimental results.

In this paper, we investigate the finite- $T$  properties of Q1D quarter-filled systems, particularly finite- $T$  phase diagrams including various charge and lattice ordered phases, by a quantum Monte Carlo method with interchain mean-field approximation. This numerical method is reliable enough to obtain high-precision results down to low  $T$  far below that previously studied by QTM. The main results are summarized in the phase diagrams in Fig. 1, which show how phase competition and coexistence are controlled by electron correlation and electron-lattice coupling. We will discuss the results in comparison with experiments on the above-mentioned compounds.

\*E-mail: otsuka@sci.u-hyogo.ac.jp

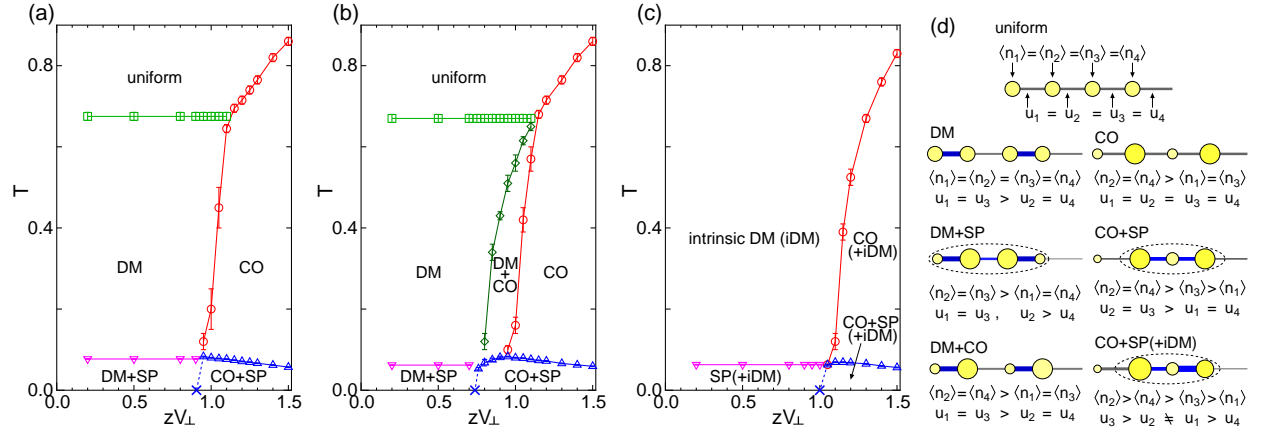


Fig. 1. Phase diagrams in the plane of  $zV_{\perp}$  and  $T$  for  $t = 1$ ,  $U = 6$ ,  $V = 2.5$ , and  $K_P = 0.75$ ; (a)  $\delta_d = 0$  and  $K_{P_2} = 0$ , (b)  $\delta_d = 0$  and  $K_{P_2} = 0.75$ , (c)  $\delta_d = 0.02$  and  $K_{P_2} = 0$ . Phase boundaries at  $T = 0$  (cross symbols) are obtained by the exact diagonalization (Lanczos) method for  $N=12$ . (d) Schematic views of different ordered states. Dashed ellipses represent spin-singlets. Note that in (c), intrinsic dimerization always exists; therefore CO(+iDM) and SP(+iDM) phases respectively have the same patterns as DM+CO and DM+SP states in (d).

Our Q1D Hamiltonian is given by  $\mathcal{H} = \sum_j \mathcal{H}_{1D}^j + \mathcal{H}_\perp$ , where  $\mathcal{H}_{1D}^j$  and  $\mathcal{H}_\perp$  represent the intrachain Hamiltonian of the  $j$ -th chain and interchain one, respectively. The intrachain part is described by the extended Hubbard model with the Peierls-type electron-lattice coupling, whose Hamiltonian reads

$$\begin{aligned} \mathcal{H}_{1D}^j = & - \sum_{i,\sigma} \{t + (-1)^i \delta_d\} (1 + u_{i,j}) (c_{i,j,\sigma}^\dagger c_{i+1,j,\sigma} + \text{h.c.}) \\ & + \frac{K_P}{2} \sum_i u_{i,j}^2 + \frac{K_{P_2}}{2} \sum_i u_{i,j}^4 \\ & + U \sum_i n_{i,j} \uparrow n_{i,j} \downarrow + V \sum_i n_{i,j} n_{i+1,j} - \mu \sum_i n_{i,j}, \end{aligned} \quad (1)$$

where the notations are referred to ref. 14. The lattice distortions  $u_{i,j}$  couple to electrons through the transfer integrals, and the coupling constant is incorporated in the definition of  $u_{i,j}$ . We treat  $u_{i,j}$  as classical variables. The elastic energy is considered up to the fourth order, where the term with  $K_{P_2}$  represents the anharmonic contribution. The interchain part is given by

$$\mathcal{H}_\perp = V_\perp \sum_{\langle j,k \rangle} \sum_i n_{i,j} n_{i,k}, \quad (2)$$

where  $V_\perp$  denotes the interchain Coulomb interaction and the summation for  $\langle j,k \rangle$  runs over nearest-neighbor chains. In the following calculations, we choose the on-site and nearest-neighbor Coulomb interactions as  $U = 6$  and  $V = 2.5$ , respectively,<sup>17</sup> and the elastic constant as  $K_P = 0.75$ , in energy unit of  $t$ . The chemical potential  $\mu$  is controlled so that the system is at quarter filling.

We derive an effective 1D model under two approximations. The first is the interchain mean-field approximation; by extending eq. (4) in ref. 14 to incorporate the CO+SP state in Fig 1(d), we assume the mean-field form of  $\mathcal{H}_\perp$  as

$$\mathcal{H}_\perp^{\text{MF}} = \frac{zV_\perp}{2} \sum_i \{(\langle n_{i-1} \rangle + \langle n_{i+1} \rangle) n_i - \langle n_{i-1} \rangle \langle n_{i+1} \rangle\}, \quad (3)$$

where  $z$  denotes the number of nearest-neighbor chains and the chain index  $j$  is dropped hereafter. The second is the adiabatic approximation for the lattice distortions; we consider the situation where the dynamics of lattices is much slower than that of electrons and fluctuations of electrons play a major role. The lattice distortions  $u_i$  are then determined so as to minimize the free energy under the constraint  $\sum_i u_i = 0$ . Note that we omit the chain index  $j$  again,  $u_{i,j} = u_i$ . These two approximations give rise to an effective 1D model  $\mathcal{H}_{1D} + \mathcal{H}_\perp^{\text{MF}}$  with self-consistent conditions for  $\langle n_i \rangle$  and  $u_i$ , which exhibits finite- $T$  phase transitions. This is suitable for our purpose, i.e., to capture the essential features of the phase transitions governed by 1D electronic fluctuations which occur at finite  $T$  assisted by the additional three-dimensionality.

We solve the effective 1D model by a quantum Monte Carlo technique called the stochastic-series-expansion (SSE) method<sup>18,19</sup> in the operator-loop-update scheme.<sup>20,21</sup> The SSE calculations fully include thermal and quantum fluctuations of electrons and give

unbiased and high-precision data for the effective 1D model. We use the expectation values by SSE in the self-consistent equations, and obtain the inputs for the next SSE calculations in turn. This cycle is repeated until the convergence is reached for all  $\langle n_i \rangle$  and  $u_i$ . We consider symmetry breaking with a four-site period along the chain by taking account of tetramerizations in the experiments, and solve the self-consistent equations for eight order parameters: four each for the charge densities  $\langle n_l \rangle$  and the lattice distortions  $u_l$  ( $l = 1, 2, 3, 4$ ). We have calculated systems with sizes up to  $N = 64$  sites and confirmed that finite-size effects are negligible down to  $T = 0.02t$ .

First, let us show the results in the absence of intrinsic dimerization, i.e.,  $\delta_d = 0$ . Figure 2 shows the  $T$ -dependences of the charge densities  $\langle n_i \rangle$ , the lattice distortions  $u_i$ , and the charge and magnetic susceptibilities  $\chi_c$  and  $\chi_s$ , in the case of the harmonic lattice ( $K_{P_2} = 0$ ). Figures 2(a)-2(c) show the results for  $zV_\perp = 1.5$ , which are typical behaviors when the interchain Coulomb interaction is dominant compared with the electron-lattice coupling, and Figs. 2(d)-2(f) show those for an opposite situation with  $zV_\perp = 0.25$ .

In the former case, CO takes place at  $T = T_{\text{CO}} \simeq 0.86$ , as observed in the alternation of  $\langle n_i \rangle$  shown in Fig. 2(a). The charge susceptibility  $\chi_c$  ( $= \partial n / \partial \mu$ ,  $n$ : average electron density) suddenly drops at  $T_{\text{CO}}$  and decreases rapidly below it owing to the opening of a charge gap, while the magnetic susceptibility  $\chi_s$  ( $= \partial m / \partial h$ ,  $m$ : average magnetic moment,  $h$ : magnetic field) show no obvious change at  $T_{\text{CO}}$ <sup>14,22</sup> [Fig. 2(c)]. This is the transition to a paramagnetic insulating state. The order parameter for CO develops down to  $T \simeq 0.3$ , below which, unexpectedly, it slightly decreases [the inset of Fig. 2(a)]. This temperature corresponds to the region where  $\chi_s$  deviates from the Curie-Weiss behavior [Fig. 2(c)], i.e., where spins start to interact with each other. Hence, we consider that this reduction of CO is due to 1D fluctuations fully taken into account in our scheme. With further decrease in  $T$ , tetramerization emerges in both the charge and bond sectors at  $T = T_{\text{CO+SP}} \simeq 0.06$ , as shown in Figs. 2(a) and 2(b), which was not accessible in the previous QTM results.<sup>14</sup> This transition is ascribed to the SP transition, where two neighboring spins at charge-rich sites form a spin-singlet pair with spontaneous lattice distortions: the low- $T$  phase is the CO+SP state<sup>17</sup> sketched in Fig. 1(d). The sudden drop in  $\chi_s$  below  $T_{\text{CO+SP}}$  in Fig. 2(c) confirms that the system has a spin gap.

Different successive transitions occur when the electron-lattice coupling is dominant [Figs. 2(d)-2(f)]. In this case, the lattice dimerization first takes place at  $T = T_{\text{DM}} \simeq 0.67$  [Fig. 2(e)], which leads the system effectively half-filled. This indicates the DM transition with the opening of a charge gap, as seen in the strong suppression of  $\chi_c$  [Fig. 2(f)].  $\chi_s$  shows no significant change at  $T_{\text{DM}}$ , and again this is characteristic of the transition to a paramagnetic insulator. Similarly to that in the CO case, the DM order parameter decreases slightly below  $T \simeq 0.2$  [the inset of Fig. 2(e)], where  $\chi_s$  deviates from the Curie-Weiss behavior [Fig. 2(f)]. Symmetry breaking with a four-site period occurs at  $T = T_{\text{DM+SP}} \simeq 0.08$ , as

shown in Figs. 2(d) and 2(e). This is another SP transition from the DM state to the DM+SP state<sup>23</sup> with a sudden drop in  $\chi_s$  [Fig. 2(f)], whose ordering pattern is different from that of the CO+SP state, as shown in Fig. 1(d).

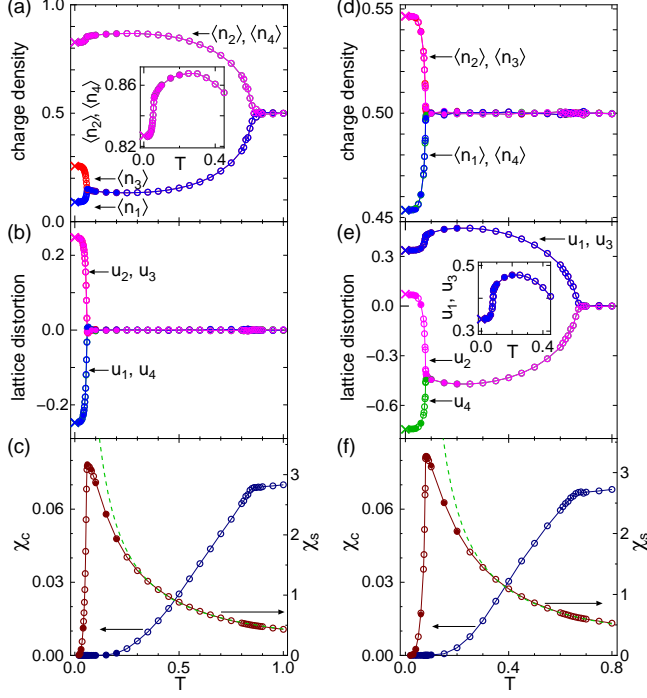


Fig. 2. Temperature dependences of charge densities, lattice distortions, and charge and magnetic susceptibilities for  $U = 6$ ,  $V = 2.5$ ,  $K_P = 0.75$ ,  $\delta_d = 0$ , and  $K_{P_2} = 0$ ; (a)-(c)  $zV_\perp = 1.5$ , (d)-(f)  $zV_\perp = 0.25$ . Open and closed circles represent results for  $N=32$  and  $64$ , respectively. Statistical errors are smaller than the symbol sizes. Data shown by cross symbols at  $T=0$  are obtained by the exact diagonalization (Lanczos) method for  $N=12$ . The dashed line in (c) [(f)] shows a Curie-Weiss fit for  $0.3 < T < T_{CO}(T_{DM})$ .

Results obtained by varying  $zV_\perp$  are summarized in the  $zV_\perp$ - $T$  phase diagram of Fig. 1(a). At high  $T$ , there are phase transitions from a high- $T$  uniform metal to intermediate- $T$  paramagnetic insulators with the two-site period, the DM or CO state; both transitions are of second order. The DM and CO states are competing with each other and the transition between them appears to be of first order. Thus, the phase diagram is likely of bicritical type as a result of this competition. We will come back to this point later. At lower  $T$ , the tetramerizations emerge upon both the CO and DM states, and these SP transitions are of second order. Note that the low- $T$  phases were not identified in the previous QTM study because of numerical limitations.<sup>14</sup>

The phase diagram is also investigated in the case of anharmonic lattice distortions, as shown in Fig. 1(b), for  $K_{P_2} = 0.75$ . The anharmonicity opens a window where DM and CO coexist, and therefore, the phase diagram shows a tetracritical behavior. Although the coexisting phase was already found in ref. 14, here we elucidate that the lattice anharmonicity is a controlling param-

eter of multicriticality. It is clear that the anharmonicity  $K_{P_2}$  stabilizes the coexistence of DM and CO. We note that the harmonic model with  $K_{P_2} = 0$  appears to be on the verge of bicritical and tetracritical behaviors,<sup>24</sup> even though it is rather difficult to exclude the coexistence in a very narrow range. Typical  $T$  dependences of the order parameters in the coexisting regime are shown in Fig. 3 for  $zV_\perp = 0.9$ . At  $T_{DM} \simeq 0.67$ , dimerization occurs first in the bond sector, and CO appears at a lower  $T_{DM+CO} \simeq 0.42$ ; CO coexists with DM below  $T_{DM+CO}$ . With further decreasing  $T$ , the degree of lattice dimerization decreases as CO grows, and finally, the system exhibits a transition to the CO+SP state. This transition appears to be of first order since the lattice dimerization suddenly vanishes as shown in Fig. 3(b). For large or small  $zV_\perp$ , the coexistence of DM and CO disappears, and the successive transitions as in Fig. 2 take place. The results are summarized in Fig. 1(b).

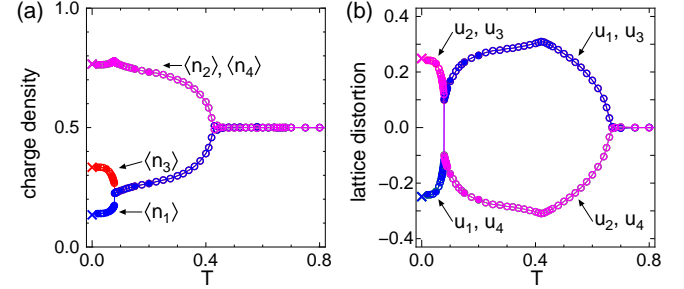


Fig. 3. Temperature dependences of (a) charge densities and (b) lattice distortions for  $U = 6$ ,  $V = 2.5$ ,  $K_P = 0.75$ ,  $\delta_d = 0$ ,  $K_{P_2} = 0.75$ , and  $zV_\perp = 0.9$ . The same symbols as those in Fig. 2 are used.

Finally, we study the effects of the intrinsic lattice dimerization  $\delta_d$ . The phase diagram for  $\delta_d = 0.02$  is represented in Fig. 1(c) and typical  $T$  dependences of physical quantities are shown in Fig. 4. For  $\delta_d \neq 0$ , there is no DM transition since the lattice dimerization is always induced even at high  $T$  [Figs. 4(b) and 4(e)]. We thus refer to the dimerized state without spontaneous symmetry breaking at high  $T$  as the intrinsic DM (iDM) state in the phase diagram in Fig. 1(c). When  $zV_\perp$  is dominant, CO and SP transitions occur similarly to the cases of  $\delta_d = 0$  as shown in Figs. 4(a) and 4(b). Note, however, that the CO+SP(+iDM) state here is slightly different from the CO+SP state for  $\delta_d = 0$  because of the underlying lattice dimerization [Fig. 1(d)]. On the other hand, when the electron-lattice coupling is dominant, CO is suppressed and the iDM state prevails until the tetramerization takes place at lower  $T$  [Figs. 4(d) and 4(e)].  $\chi_s$  behaves similarly to that for  $\delta_d = 0$  in both cases [Figs. 4(c) and 4(f)], indicating that the intrinsic lattice dimerization have no significant effect on the spin sector. On the other hand,  $\chi_c$  behaves differently at high  $T$ : it is suppressed even at  $T > T_{CO}$  because of the Mott insulating nature of the iDM state. The phase diagram is summarized in Fig. 1(c), where the DM transition is absent and the phase transition between the iDM and



CO(+iDM) phases is of second order.

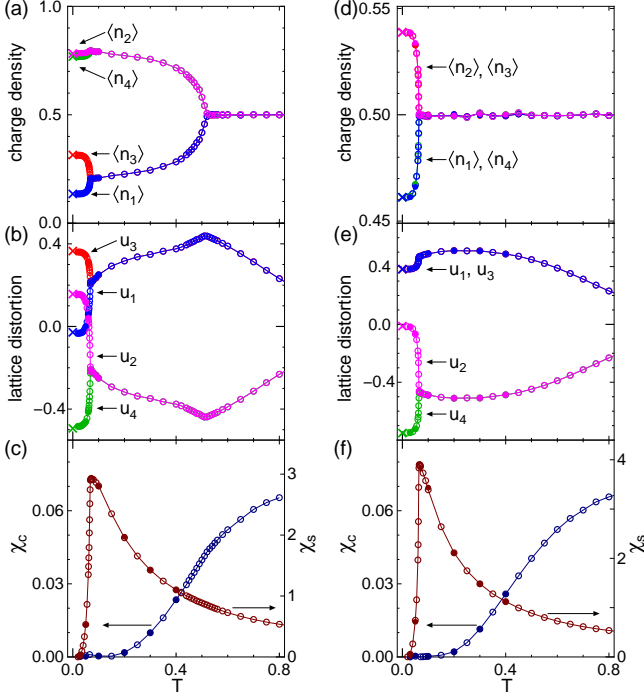


Fig. 4. Temperature dependences of charge densities, lattice distortions, and charge and magnetic susceptibilities for  $U = 6$ ,  $V = 2.5$ ,  $K_P = 0.75$ ,  $\delta_d = 0.02$ , and  $K_{P_2} = 0$ ; (a)-(c)  $zV_\perp = 1.2$ , (d)-(f)  $zV_\perp = 0.2$ . The same symbols as those in Fig. 2 are used.

Now let us discuss our results in comparison with the experimental data. The family of  $(R_1R_2\text{-DCNQI})_2X$  has uniform DCNQI chains at high  $T$ , corresponding to the cases of  $\delta_d = 0$  in our model. The successive transitions with dimerization and tetramerization observed in DMe-DCNQI<sub>2</sub>Ag<sup>5</sup> are reproduced by the DM and SP transitions, as shown in Figs. 2(d)-2(f). The CO transition in DI-DCNQI<sub>2</sub>Ag<sup>4</sup> is also reproduced in Figs. 2(a)-2(c), but the low- $T$  antiferromagnetism<sup>3</sup> is out of the scope of our model because we neglect the interchain hopping that results in an effective antiferromagnetic exchange interaction between chains.<sup>25</sup> On the other hand, (TMTTF)<sub>2</sub> $X$  has an intrinsic dimerization, and hence corresponds to  $\delta_d \neq 0$ . The CO and SP transitions observed for  $X = \text{PF}_6$  and  $\text{AsF}_6$  are reproduced in Figs. 4(a)-4(c). Furthermore, our phase diagram in Fig. 1(c) shows a good agreement with the  $P$ - $T$  phase diagram for  $X = \text{AsF}_6$ <sup>8</sup> when we read the interchain Coulomb interaction  $zV_\perp$  as the inverse of  $P$ . This is reasonable since the pressure is supposed to increase mainly the intrachain transfer integrals, i.e., to effectively decrease the interchain interaction. As to the pressure effect on DCNQI compounds, the case for DMe-DCNQI<sub>2</sub>Ag has not been explored yet, but it was shown that DI-DCNQI<sub>2</sub>Ag exhibits a peculiar tricritical behavior under  $P$ .<sup>26</sup> Although we have found no tricritical point in Figs. 1(a) and 1(b), our observation of the role of lattice anharmonicity in the multicriticality indicates the possibility of capturing such behavior by

extending our model, particularly in the electron-lattice part.

It should be pointed out that the obtained phase diagrams will be modified if we go beyond the interchain mean-field or adiabatic approximation. For example, the effects of fluctuations and quantum nature in the lattice are anticipated to contract the DM and SP phases. These phases would nevertheless survive at finite  $T$  provided that three-dimensional lattice couplings are included. Hence, we presume that the general features of our phase diagrams remain robust, and bear the comparisons with experiments. The effects of fluctuations neglected in the present calculations are left for future study.

In summary, we have investigated the finite-temperature phase transitions in quasi-one-dimensional quarter-filled systems using the extended Hubbard model with electron-lattice coupling. The effective one-dimensional model, obtained by interchain mean-field approximation, has been numerically solved by the stochastic-series-expansion Monte Carlo method down to temperatures far below that previously studied. A variety of phase diagrams have been explored and rich behaviors of competition and coexistence have been clarified among charge, lattice and spin degrees of freedom. We have found that an anharmonicity of lattice distortions is a key parameter of multicritical behaviors. Our results reproduce well the charge ordering, dimer Mott, and spin-Peierls states in DCNQI and TMTTF compounds.

## Acknowledgments

The authors thank S. E. Brown, R. T. Clay, S. Fujiyama, H. Yoshioka, and M. Tsuchiizu for fruitful discussions. This work is supported by Grants-in-Aid for Scientific Research (Nos. 18028018, 18028026, 19014020) from the Ministry of Education, Culture, Sports, Science and Technology, and by Next Generation Integrated Nanoscience Simulation Software.

- 1) For recent reviews, Chem. Rev. **104** (2004) No. 11, Issue on Molecular Conductors; J. Phys. Soc. Jpn. **75** (2006) No. 5, Special Topics Session on Organic Conductors.
- 2) T. Miyazaki and K. Terakura: Phys. Rev. B **54** (1996) 10452.
- 3) K. Hiraki and K. Kanoda: Phys. Rev. B **54** (1996) R17276.
- 4) K. Hiraki and K. Kanoda: Phys. Rev. Lett. **80** (1998) 4737.
- 5) R. Moret, P. Erk, S. Hünig, and J. U. Von Schütz: J. Phys. (Paris) **49** (1988) 1925.
- 6) D. Jérôme: Chem. Rev. **104** (2004) 5565.
- 7) D. S. Chow, F. Zamborszky, B. Alavi, D. J. Tantillo, A. Baur, C. A. Merlic, and S. E. Brown: Phys. Rev. Lett. **85** (2000) 1698.
- 8) F. Zamborszky, W. Yu, W. Raas, S. E. Brown, B. Alavi, C. A. Merlic, and A. Baur: Phys. Rev. B **66** (2002) R081103.
- 9) W. Yu, F. Zhang, F. Zamborszky, B. Alavi, A. Baur, C. A. Merlic, and S. E. Brown: Phys. Rev. B **70** (2004) 121101.
- 10) For review, H. Seo, J. Merino, H. Yoshioka, and M. Ogata: J. Phys. Soc. Jpn. **75** (2006) 051009.
- 11) M. Sugiura, M. Tsuchiizu, and Y. Suzumura: J. Phys. Soc. Jpn. **73** (2004) 2487.
- 12) M. Sugiura, M. Tsuchiizu, and Y. Suzumura: J. Phys. Soc. Jpn. **74** (2005) 983.
- 13) H. Yoshioka, M. Tsuchiizu, and H. Seo: J. Phys. Soc. Jpn. **75** (2006) 063706.
- 14) H. Seo, Y. Motome, and T. Kato: J. Phys. Soc. Jpn. **76** (2007) 013707.

- 15) R. T. Clay, R. P. Hardikar, and S. Mazumdar: Phys. Rev. B **76** (2007) 205118.
- 16) H. Yoshioka, M. Tsuchiizu, and H. Seo: J. Phys. Soc. Jpn. **76** (2007) 103701.
- 17) M. Kuwabara, H. Seo, and M. Ogata: J. Phys. Soc. Jpn. **72** (2003) 225.
- 18) A. W. Sandvik and J. Kurkijärvi: Phys. Rev. B **43** (1991) 5950.
- 19) A. W. Sandvik: J. Phys. A **25** (1992) 3667.
- 20) A. W. Sandvik: Phys. Rev. B **59** (1999) R14157.
- 21) P. Sengupta, A. W. Sandvik, and D. K. Campbell: Phys. Rev. B **65** (2002) 155113.
- 22) Y. Tanaka and M. Ogata: J. Phys. Soc. Jpn. **74** (2005) 3283.
- 23) K. C. Ung, S. Mazumdar, and D. Toussaint: Phys. Rev. Lett. **73** (1994) 2603.
- 24) We also found that the anharmonicity changes the multicritical behaviors between tetramized SP phases, which will be discussed elsewhere.
- 25) J. Riera and D. Poilblanc: Phys. Rev. B **62** (2000) R16243.
- 26) T. Itoh, K. Kanoda, K. Murata, T. Matsumoto, K. Hiraki, and T. Takahashi: Phys. Rev. Lett. **93** (2004) 216408.